Modeling of a Cascaded Raman Laser in Mid-IR

V. M. N. Passaro[1] and F. De Leonardis[2]

[1] Politecnico di Bari, Dipartimento di Elettrotecnica ed Elettronica, via E. Orabona 4, 70125 Bari, Italy
[2] Politecnico di Bari, Dipartimento di Ingegneria dell'Ambiente e per lo Sviluppo Sostenibile, viale del Turismo 8, 74100 Taranto, Italy

In this work a non linear coupled-mode model is applied to design a cascaded Raman laser in mid-IR, based on silicon-on-insulator technology. The laser architecture is formed by a resonant microcavity and the pump power is injected by evanescent coupling from an external SOI bus waveguide. A number of higher order Stokes waves are then generated inside the microcavity by SRS, with different wavelengths extending in the mid-IR region (above 3 µm). Lasing thresholds are optimized for quasi-TM modes, showing as low as 13 mW and 50 mW for first and second order Stokes waves, respectively, and lasing output of about 7 mW.

Introduction

In recent years, mid-infrared (mid-IR) sources have found use in a wide array of applications ranging from purely scientific uses, to clinical and industrial ones, such as tissue ablation, hydrocarbon detection, environment monitoring. Several studies have been developed towards distributed feedback quantum cascade lasers to achieve low threshold mid-IR sources. More recently, another approach, based on Stimulated Raman Scattering (SRS) effect, has been considered as a promising candidate to realise efficient mid-IR light sources. In fact, one of the major advantages of Raman lasers is their relative ability to generate coherent light in wavelength regions that are not easily accessible with other types of lasers. Therefore, in this work we show the theoretical model to design a cascaded Raman laser in the mid-IR based on silicon-on-insulator technology.

Numerical analysis

In our analysis we assume the architecture as sketched in Fig. 1, where the input pump (S_p) is injected in the resonant microcavity by the evanescent coupling from an external SOI bus waveguide.

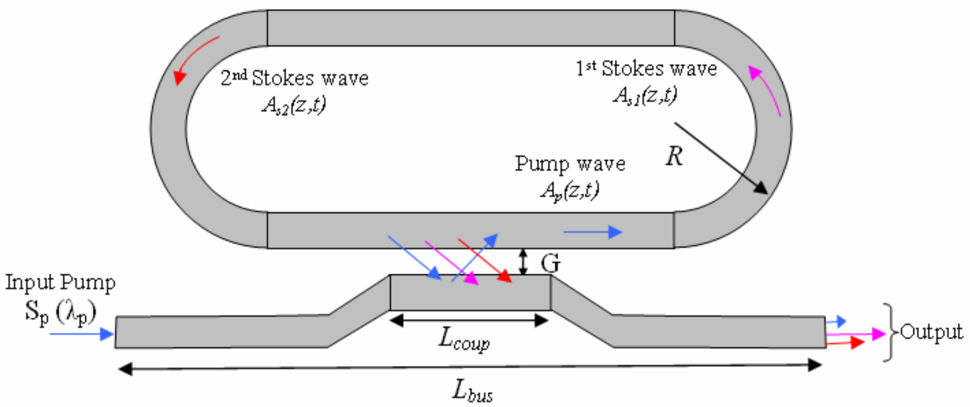

Fig. 1. Architecture of mid-IR Raman laser, based on a resonant microcavity.

The pump coupled into the laser cavity generates optical gain by SRS inside the silicon waveguide at first-order Stokes wavelength. The optical power of this first-order Stokes wave starts to increase inside the cavity, inducing a pump depletion and eventually gain for the second-order Stokes signal, whose wavelength will be shifted from the first-order wave by Raman shift (15.6 THz in silicon). This cascaded process can continue and generate higher-order Stokes lasing at longer wavelengths. The differential equation system governing this power coupling among different waves is rather complicated, even because both polarizations (quasi-TE and quasi-TM) are in general excited in SOI waveguides. Here we give the differential equation governing the space-time evolution of both first and second order Stokes waves propagating inside the cavity. Then, we have for quasi-TE and quasi-TM first ($\kappa = 3,4$) and second order Stokes ($\kappa = 5,6$) pulses:

$$
\begin{aligned}
& v_{g,\kappa}\frac{\partial A_\kappa}{\partial z} + \frac{\partial A_\kappa}{\partial t} + j v_{g,\kappa}\frac{1}{2}\beta_{2,\kappa}\frac{\partial^2 A_\kappa}{\partial t^2} - v_{g,\kappa}\frac{1}{6}\beta_{3,\kappa}\frac{\partial^3 A_\kappa}{\partial t^3} = j(\bar{\omega}_\kappa - \omega_\kappa)A_\kappa - \frac{1}{2}\frac{1}{\tau_\kappa}A_\kappa + j2v_{g,\kappa}\gamma_{\kappa,\mu}\left|A_\mu\right|^2 A_\kappa + \\
& + j2v_{g,\kappa}\gamma_{\kappa,\mu+1}\left|A_{\mu+1}\right|^2 A_\kappa + j v_{g,\kappa}\gamma_{\kappa,\kappa}\left|A_\kappa\right|^2 A_\kappa + j2v_{g,\kappa}\gamma_{\kappa,\nu}\left|A_\nu\right|^2 A_\kappa + \frac{1}{2}v_{g,\kappa}g_{R,\kappa}f_{\kappa,\mu}\left|A_\mu\right|^2 A_\kappa + v_{g,\kappa}\frac{1}{2}g_{R,\kappa}f_{\kappa,\mu+1}\left|A_{\mu+1}\right|^2 A_\kappa + \\
& + j2v_{g,\kappa}k_{\kappa,\mu,\mu+1,\nu}A_{\mu+1}A_\mu^* A_\nu e^{j(\bar{k}_{\mu+1}+\bar{k}_\nu-\bar{k}_\mu-\bar{k}_\kappa)z} + j2v_{g,\kappa}k_{\kappa,\mu+1,\mu,\nu}A_\mu A_{\mu+1}^* A_\nu e^{j(\bar{k}_\mu+\bar{k}_\nu-\bar{k}_{\mu+1}-\bar{k}_\kappa)z} + j v_{g,\kappa}k_{\kappa,\kappa,\nu,\nu}A_\nu A_\kappa^* A_\nu e^{j(2\bar{k}_\nu-2\bar{k}_\kappa)z} + \\
& - \frac{1}{2}v_{g,\kappa}g_{R,\kappa}f_{\kappa,\mu+4}\left|A_{\mu+4}\right|^2 A_\kappa - \frac{1}{2}v_{g,\kappa}g_{R,\kappa}f_{\kappa,\mu+5}\left|A_{\mu+5}\right|^2 A_\kappa + j2v_{g,\kappa}k_{\kappa,\mu+4,\nu,\mu+5}A_\nu A_{\mu+4}^* A_{\mu+5}e^{j(\bar{k}_\nu+\bar{k}_{\mu+5}-\bar{k}_\kappa-\bar{k}_{\mu+4})z} \\
& + j2v_{g,\kappa}k_{\kappa,\mu+5,\nu,\mu+4}A_\nu A_{\mu+5}^* A_{\mu+4}e^{j(\bar{k}_\nu+\bar{k}_{\mu+4}-\bar{k}_\kappa-\bar{k}_{\mu+5})z}
\end{aligned}
$$

where β_2 is the GVD coefficient, β_3 is the TOD coefficient and g_R is the Raman gain. Fig. 2 shows the comparison between experimental data proposed in [1] and modeling of this work in terms of CW cascaded Raman emission versus input pump power ($\lambda_p = 1.55$ µm, $\lambda_{s1} = 1.686$ µm, $\lambda_{s2} = 1.848$ µm). The plots show a very good agreement with experimental data in terms of threshold values, output powers above threshold, external efficiencies and output saturation. In particular, the high agreement with first Stokes output saturation confirms how the Raman cascaded lasing is well described by the mathematical model proposed in this work.

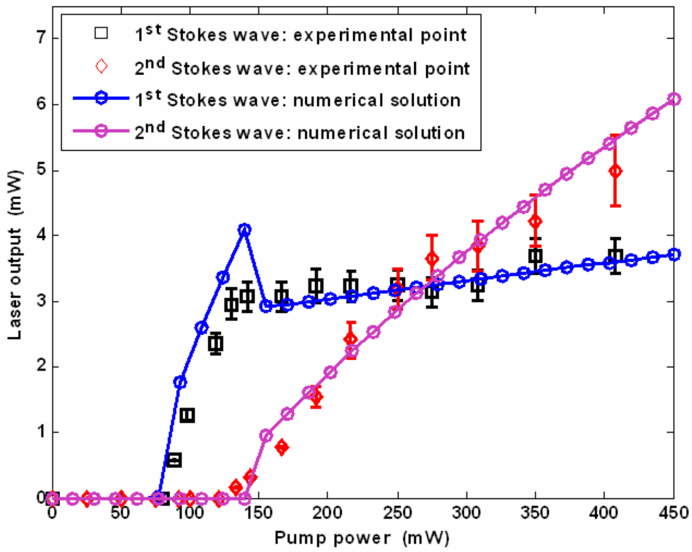

Fig. 2. Comparison between experimental data [1] and modeling of this paper in terms of CW cascaded Raman emission versus input pump power

Generally speaking, the architecture design criteria involve the waveguide cross-section, the minimum cavity length and the coupling factor. In the following simulations, the optimal waveguide cross section has been designed to definitely avoid any walk-off effect, even under pulsed regime. Then, SRS effect induced in the resonant microcavity could be only limited by the enhancement factor of the pump wave. In addition, the minimum cavity length has been set to 1 cm in order to avoid the nonlinear birefringence effect. Another very important aspect is to find the design guidelines for the directional coupling. In our cascaded Raman laser, design criteria for directional coupling are oriented to achieve polarization selectivity and output power extraction of the same order of magnitude for the first and second-order Stokes waves.
Fig. 3 shows the output of designed cascaded Raman laser operating in CW regime. Several comments are worthy to give. First, quasi-TE second-order Stokes wave presents a large value of lasing threshold, thus it cannot be lasing with an input power less than 150 mW. On the contrary, quasi-TM second-order Stokes presents similar lasing threshold and external output efficiency, independently from the polarization state of exciting first order Stokes. It seems very interesting the first-order Stokes wave lasing. In fact, in this case the coupling factors for quasi-TE and quasi-TM polarizations do not represent a discriminating factor for the threshold level, since it has the same order of magnitude. In any case, above threshold (equal for both polarizations) quasi-TM mode presents an output power level and an external efficiency larger than that for quasi-TE mode, as induced by smaller core area and larger coupling factor. Thus, lasing thresholds are optimized for quasi-TM modes, showing as low as 13 mW and 50 mW for first and second order Stokes waves, respectively, and lasing output of about 7 mW As a conclusion, quasi-TM polarization should be well suitable for simultaneous lasing of the first two Stokes waves.

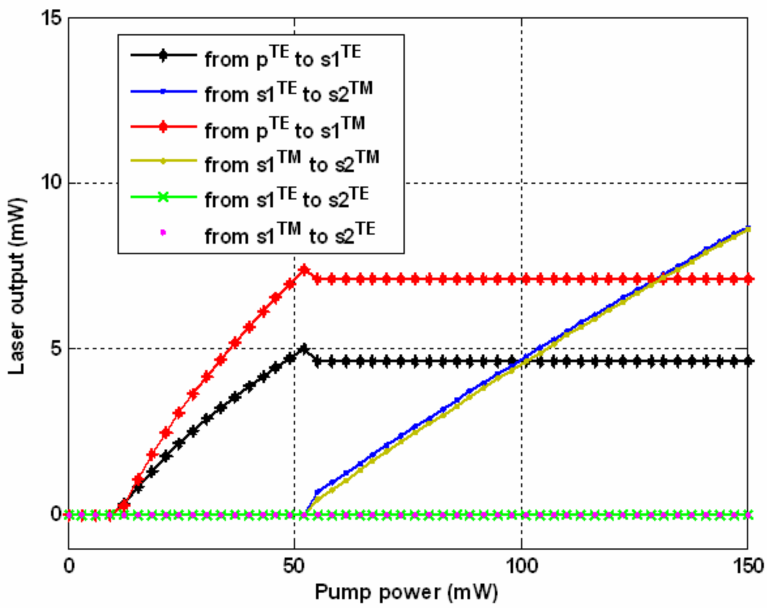

Fig. 3. Laser output versus pump power for different combinations of polarization states.

To complete the description of the theoretical behaviour of the double emission Raman laser, Fig. 4 shows the laser time dynamics under an input power condition of 131.25 mW. It is worth to note as the time reference is assumed moving with the waves, and the designed cascaded Raman laser operates in continuous-wave regime. The simulations demonstrate that not only the cascaded Raman lasing can be achieved in SOI waveguides working at mid-IR, but also that its performance are very interesting in terms of reduced power consumption, stability, wavelength tunability and polarization selectivity. In addition, our theoretical investigations have shown the possibility to obtain output power of 7.136 mW, well larger than 0.2 mW as mentioned in [2], with consequent positive impact on the electronic signal processing.

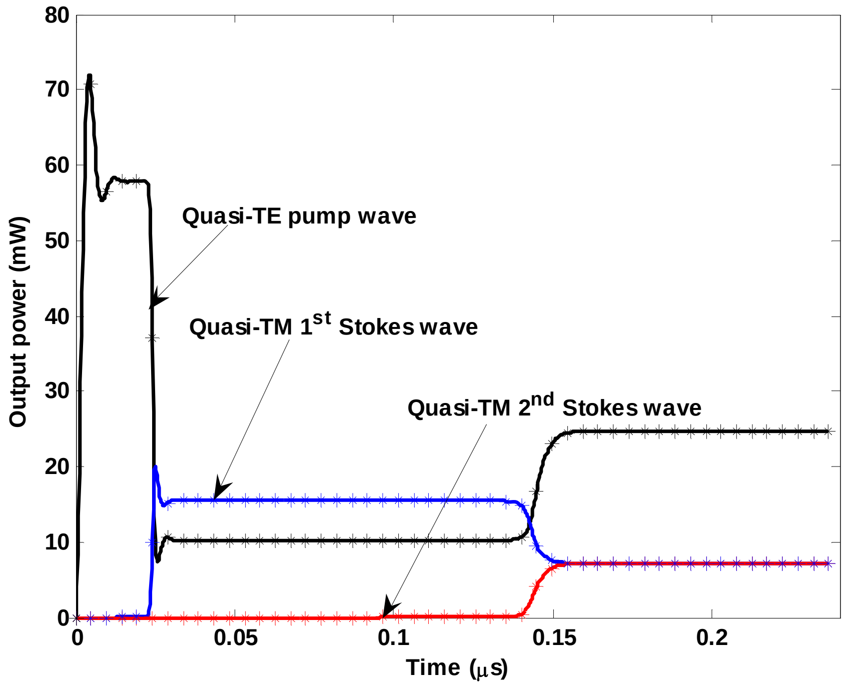

Fig. 4. Time dynamics for both pump and Stokes waves
(λ_p = 2.8519 μm, λ_{s1} = 3.3485 μm, λ_{s2} = 4.0544 μm).

The specific design of this cascaded Raman laser in CW regime could be suitable for gas sensing of two different gases having an absorption peak in mid-IR wavelength range, e.g. C_2H_6 and CO_2, as well as for gas sensing at longer mid-IR wavelengths.

References

[1] H. Rong, S. Xu, O. Cohen, O. Raday, M. Lee, V. Sih and M. Paniccia, "A cascaded silicon Raman laser", Nature Photonics, vol. 2, 170-174, 2008.

[2] O. Tadanaga, T. Yanagawa and M. Asobe, "Mid-infrared Wavelength Conversion Laser for Highly Sensitive Gas Detection", NTT Technical Review, vol. 7, 1-6, 2009.